



LAWRENCE
LIVERMORE
NATIONAL
LABORATORY

Experiment vs. theory on electric inhibition of fast electron penetration of targets

R. R. Freeman, K. U. Akli, D. Batani, S. Baton, S. P. Hatchett, D. Hey, M. H. Key, J. A. King, A. J. MacKinnon, P. A. Norreys, R. A. Snavely, R. Stephens, C. Stoeckl, R. P. J. Town, B. Zhang

June 22, 2005

32nd EPS Plasma Physics conference
tarragona, Spain
June 27, 2005 through July 1, 2005

Disclaimer

This document was prepared as an account of work sponsored by an agency of the United States Government. Neither the United States Government nor the University of California nor any of their employees, makes any warranty, express or implied, or assumes any legal liability or responsibility for the accuracy, completeness, or usefulness of any information, apparatus, product, or process disclosed, or represents that its use would not infringe privately owned rights. Reference herein to any specific commercial product, process, or service by trade name, trademark, manufacturer, or otherwise, does not necessarily constitute or imply its endorsement, recommendation, or favoring by the United States Government or the University of California. The views and opinions of authors expressed herein do not necessarily state or reflect those of the United States Government or the University of California, and shall not be used for advertising or product endorsement purposes.

This work was performed under the auspices of the U. S. Department of Energy by the University of California, Lawrence Livermore National Laboratory, under Contract No. W-7405-Eng.-48.

Experiment vs. Theory on Electric Inhibition of Fast Electron Penetration of Targets

R.R. Freeman^{1,2}, K. Akli², D. Batani³, S. Baton⁴, S. Hatchett⁵, D. Hey², M. Key⁵, J. King²
A. MacKinnon⁵, P. Norreys⁶, R. Snavely⁵, R. Stephens⁷, C. Stoeckl⁸, R. Town⁵, B. Zhang²

¹ *The Ohio State University, Columbus, OH, USA*

² *University of California-Davis, Davis, CA, USA*

³ *Departimento di Fisica "G. Occhialini", Universita' di Milano Bicocca, Milano, Italy*

⁴ *LULI, Ecole Polytechnique, Palaiseau, France*

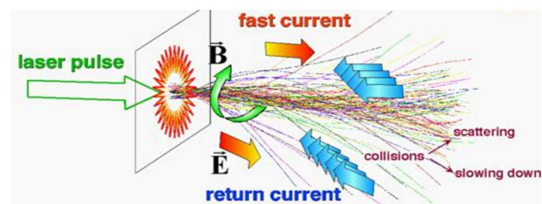
⁵ *The University of California, LLNL, Livermore, CA, USA*

⁶ *Rutherford Appleton Laboratories, Didcot, Oxfordshire, UK*

⁷ *General Atomics, San Diego, CA, USA*

⁸ *Laboratory for Laser Energetics, Rochester, NY, USA*

A dominant force of inhibition of fast electrons in normal density matter is due to an axially directed electrostatic field (Fig. 1). Fast electrons leave the critical density layer and enter the solid in an assumed relativistic Maxwellian energy distribution. Within a cycle of the solid density plasma frequency, the charge separation is neutralized by a background return current density $j_b = en_b v_b$ equal and opposite to the fast electron current density $j_f = en_f v_f$ [1] where it is assumed that the fast electron number density is much less than the background number density, $n_f \ll n_b$ [2]. This charge and current neutralization allows the forward moving fast electron current to temporarily exceed the Alfvén limit by many orders of magnitude [3]. During this period the cold return current, in passing through the material resistivity, ohmically generates an electric field in opposition to the fast current. As a result, the fast electron current loses its energy to the material, via the return current, in the form of heat [4]. So, although the highly energetic electrons suffer relatively little direct collisional loss of energy (owing to the inverse relation of the Coulomb cross section to velocity), their motion is substantially damped by ohmic heating of the slower return current. The equation for the ohmically generated electric



Hybrid PIC model (Paris) C. Toupin et al. In *Inertial Fusion Science and Applications 99* Publ. Elsevier p471 (2000)

Figure 1: Fast electrons generated at the critical density pass into the solid. Charge neutralization results in an equal and opposite return current density. Electric and magnetic fields act to inhibit fast electron penetration into the solid and deposit the energy into the material as heat.

field, E , is given by Ohm's law, $E = j_c \eta$ where η is the material resistivity .

The material resistivity, η , is a function of the material temperature and so as the current channel is ohmically heated by the slow counter-propagating electrons, η changes. In general, the variation of resistivity with temperature and density can be divided into two regimes of temperature [5]. As shown in figure 2, at low temperatures the resistivity rises linearly with temperature and plateaus at $2 \mu \Omega \text{ m}$ in the range of 10 to 100 eV for most all materials. In this cold "classical" regime, the resistivity is dominated by the collision frequency of the electrons with the background ions and the plateaus correspond to electron minimum scattering lengths comparable to the interatomic spacing [6]. Notice also that in this regime the resistivity has a strong inverse dependence on the density. At temperatures beyond the plateau, the $T^{-3/2}$ dependence of the Coulomb cross section for electron-ion scattering begins to dominate and the resistivity diminishes with temperature. In this so called "Spitzer" regime, the resistance is a very weak function of density.

Electron transport experiments were conducted at the Vulcan laser within the Rutherford Appleton Laboratory in the UK. An 81J, 800fs 1053nm Nd:glass laser pulse was focused to $10 \mu\text{m}$ by an $f/3$ off-axis parabolic mirror onto the thin edge of a solid 50/50 amalgam of Cu and Al as shown in figure 3. The laser spot was positioned $50 \mu\text{m}$ from the edge on the observation side. A 1.6 cm apertured SiO₂ 2131 quartz crystal, bent to a radius of 38 cm and operating at 1.3° off normal incidence, transversely viewed Cu $K\alpha$ x-rays from the Cu/Al amalgam and produced a 7.9x magnified image onto a Princeton Instruments, 1 square inch, 1024×1024 pixel CCD internally cooled to -30 C . Astigmatism and spherical aberration limited spatial resolution to $10 \mu\text{m}$.

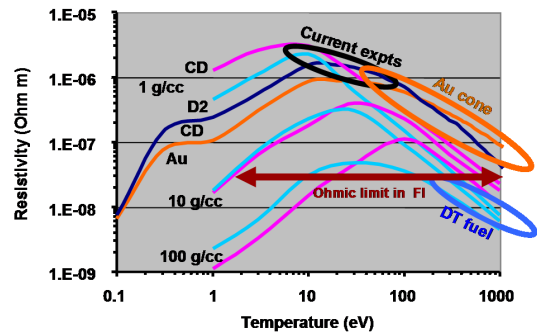


Figure 2: Plot of resistivity vs. temperature showing resistivity increasing to a universal plateau from 10 to 100 eV. At higher temperatures, in the Spitzer regime, the resistivity falls off as $T^{-3/2}$.

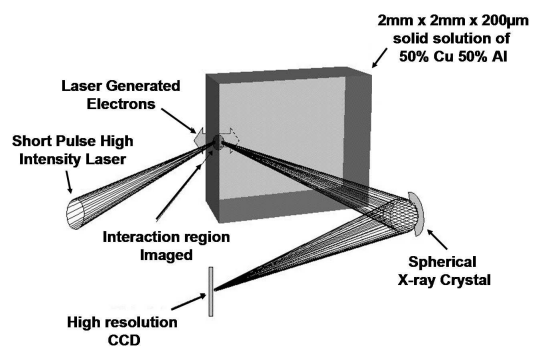


Figure 3: The diagnostic consisted of a spherically bent crystal used to image the Cu $K\alpha$ X-rays from the Cu/Al amalgam onto a CCD. The view was rotated 53° from the laser axis and the electron flow.

A typical image from these experiments is shown in figure 4. The laser was normally incident to the thin edge of the target and rotated 53° from the viewing axis. The image shows very shallow fast electron spreading into a $90\ \mu\text{m}$ spot and strongly attenuated penetration into the solid. The viewing angle combined with an assumed 40° deep spreading of the fast electrons [7] exaggerates the attenuation somewhat. The images were therefore processed to account for these effects so that, for example, the $32\ \mu\text{m}$ $1/e$ length attenuation of intensity recorded in the image of figure 4 represents an actual $1/e$ length of about $100\ \mu\text{m}$. These results of near-surface spreading and strong attenuation are consistent with findings in the rear-view buried-layer $K\alpha$ studies of Stephens *et al* [7].

An image of a shot similar to the previous except with a gold cone attached to guide the laser is shown in figure 5. The cone tip was attached with the cone axis normal to the thin edge at a distance of $50\ \mu\text{m}$ from the observation side for comparison with the no-cone shots previously discussed. The $500\ \mu\text{m}$ long cone opened from a $\leq 30\ \mu\text{m}$ hole at the tip with an angle large enough to accommodate the converging pulsed beam. Comparison of the two images in figures 4 and 5 indicates that the near-surface fast electron spreading and fast electron penetration depth are essentially identical and that the cone has no effect on the transport in this regard. It is also seen from the associated color bars that the signal level of the cone shot is much lower than that of the no-cone shot. This is most likely due to clipping of the intensity wings by the $30\ \mu\text{m}$ hole at the cone tip.

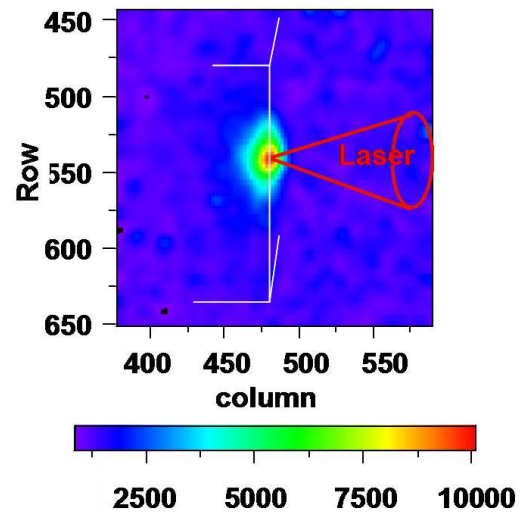


Figure 4: CCD image of Cu $K\alpha$ from a solid Cu/Al amalgam. At 53° from the laser axis, the image provides a semi-transverse view of the electron flux within the solid.

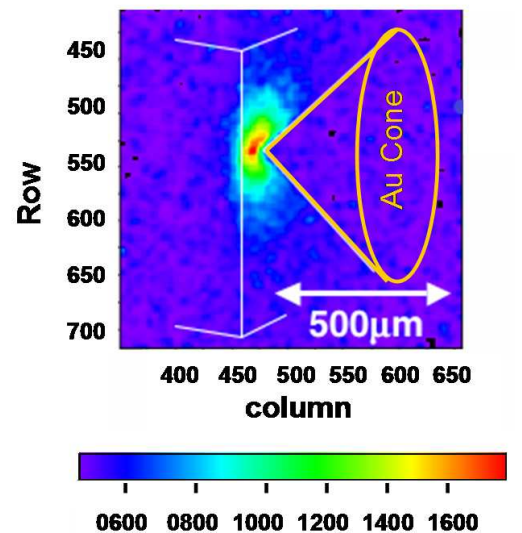


Figure 5: In this image of an otherwise identical shot, a Au cone has been attached to guide the laser pulse. Electron surface spreading and transport inhibition is the same as for the no-cone image.

With laser intensities of approximately 10^{20} W/cm² and resulting average electron energies on the order of 1 MeV, collisional stopping alone cannot account for the observed fast electron attenuation lengths of ~ 100 μ m as determined in the above images. Electric inhibition, therefore, has been invoked as a probable explanation for this strong attenuation. Indeed, as indicated in figure 2, the normal densities and 10-20 eV temperatures of the materials shot in this experiment maximize the resistivity and thus maximize the electric inhibition. In fact, all FI-related experiments on electron transport to date have been near the highest possible value of resistivity in the classical regime [8]. In contrast, full scale fast ignition transport will be within high density (300 g/cm³), high temperature (~ 1 keV) cores [10] which, as seen in figure 2, have resistivities lower by two orders of magnitude in the Spitzer regime. Furthermore, it has been predicted in modeling studies [11] that for materials initially in the Spitzer regime, low resistivity channels form due to the ohmic heating. In this case, electric inhibition is further reduced and magnetic collimation dominates over collisional/ohmic spreading to produce a tightly collimated beam.

It has been suggested that the very large initial source size consistently observed in our experiments could be attributed to a non-ideal spatial profile of the beam. Unlike an ideal Gaussian beam whose intensity falls off quickly in the radial direction, a real beam falls off slowly with non-negligible intensity in its wings. In this experiment, that hypothesis has been tested by the addition of gold cones. If the 90 μ m diameter spot size observed in the no-cone shot were due to the laser intensity profile, then adding a cone with a small 30 μ m diameter hole at its tip would clip this intensity resulting in a much smaller source diameter. However, as seen by comparison of figures 4 and 5, there is no significant reduction in source spread with the use of a cone and therefore it appears that the spreading is not due to the laser intensity profile.

One possible physical mechanism for source spreading is a radially directed force due to crossed **E** and **B** fields within the pre-plasma [9]. The **E** field, which is normal to the surface, results from a pre-pulse generated charge non-neutral hydrodynamic "blow off" and the azimuthal **B** field results from the crossed gradients of the longitudinally increasing density and radially decreasing temperature.

In conclusion, penetration depth and surface spreading as determined from transverse Cu K α imaging of Cu/Al amalgam targets are in good agreement with rear-surface K α imaging studies. In all experiments so far, electron transport has been dominated by electric inhibition and until higher temperature, higher density experiments are accessible, it may be feasible for transport studies to go to lower temperature, higher density shocked materials in which the resistivity is decreased and higher penetration is possible. The possibility of surface spreading due to the non-

negligible intensity within the wings of non-ideal laser intensity profiles has been eliminated. Spreading is now thought to be a result of crossed \mathbf{E} and \mathbf{B} fields which develop within the pre-plasma. While perhaps within this presentation there have been no new unexplained physical mechanisms to speak of, it is important to communicate that experimental observations thus far have been consistent with the dominance of electric inhibition and $\mathbf{E} \times \mathbf{B}$ surface spreading.

References

- [1] A. Bell, J. Davies, S. Guerin, and H. Ruhl, *Plasma Phys. Control Fusion* **39**, 653 (1997)
- [2] D. Hammer and N. Rostoker, *Phys. Fluids* **13**, 1831 (1970)
- [3] J. Davies, *Phys. Rev. E* **68**, 056404 (2003)
- [4] J. Davies, A. Bell and M. Haines *Phys. Rev. E* **56**, 7193 (1997)
- [5] H. Milchberg, R. Freeman and S. Davey *Phys. Rev. Lett.* **61**, 2364 (1988)
- [6] Y. Lee and R. More, *Phys. Fluids* **27**, 1273 (1984)
- [7] R. Stephens et al, *Phys. Rev. E* **69**, 066414 (2004)
- [8] R. Freeman, et al (to be published)
- [9] D. Forslund and J. Brackbill, *Phys. Rev. Lett.* **61**, 2364 (1988)
- [10] M. Tabak et al, *Phys. Plasmas* **1**, 1626 (1994)
- [11] J. Davies, A. Bell and M. Tatarakis, *Phys. Rev. E* **59**, 6032 (1999)